Influences of hydrostatic pressure during casting and Pd content on as-cast phase in Zr-Al-Ni-Cu-Pd bulk alloys

doi: 10.1063/1.1790028

Influences of hydrostatic pressure during casting and Pd content on as-cast phase in Zr-Al-Ni-Cu-Pd bulk alloys

Hidemi Kato and Akihisa Inoue
Institute for Materials Research, Tohoku University Katahira 2-1-1, Sendai 980-8577, Japan

Junji Saida
Center for Interdisciplinary Research, Tohoku University Aramaki, Aoba, Sendai 980-8578, Japan

(Received 20 April 2004; accepted 7 July 2004)

The influences of sample diameter (D), Pd content (x), and hydrostatic pressure (P) in a chamber during casting on the structure of as cast $Zr_{65}Al_{7.5}Ni_{10}Cu_{17.5-x}Pd_x$($x=10, 17.5$ at.%) bulk alloys were investigated. $Zr_{65}Al_{7.5}Ni_{10}Cu_{7.5}Pd_{10}$ and $Zr_{65}Al_{7.5}Ni_{10}Pd_{17.5}$ alloys ($D=3$ mm) cast in a vacuum chamber ($P\sim 4.0\times 10^{-3}$ Pa) were mainly of the tetragonal-Zr_2Ni equilibrium phase and nanosize icosahedral primary phase, respectively, while the same alloys cast in inert argon gas at atmospheric pressure ($P\sim 0.1$ MPa) were of the single glassy phase. Due to the higher cooling rate obtained by decreasing the sample diameter ($D=2$ mm) even in the vacuum chamber, the $Zr_{65}Al_{7.5}Ni_{10}Pd_{17.5}$ alloy was still of the icosahedral phase, while the $Zr_{65}Al_{7.5}Ni_{10}Cu_{7.5}Pd_{10}$ alloy froze into a single glassy phase. These results indicate that the temperature- and time-transformation curves for the icosahedral and subsequent equilibrium phase formations in the alloy system shifts to a shorter time side with decreasing P, and the pressure sensitivity of the icosahedral phase formation increases with x. © *2004 American Institute of Physics*. [DOI: 10.1063/1.1790028]

The precipitation of an icosahedral quasicrystalline (QC) phase as primary crystallization was observed in melt-spun ribbons of Zr-based multicomponent systems with several additives such as noble metals (NM=Ag, Pd, Au, or Pt)[1,2] and oxygen.[3] In Zr-TM-NM(TM=Fe, Co, Ni, or Cu)[4,5] ternary systems, QC phase precipitation was also observed. Moreover, QC phase precipitation was also discovered in binary Zr-Pd and Zr-Pt ribbons even in the quenched state.[6] Therefore, NM and TM elements are considered the dominant and stabilizing factors of QC phase formation, respectively. From these and other previous reports, Murty and Hono demonstrated the schematic classification of alloy systems based on the QC phase-forming tendency and glass forming ability (GFA) using a temperature-time-transformation (TTT) diagram.[7] The illustration indicates that QC phase precipitation in bulk metallic glasses should be determined by the relationship between the cooling route and the TTT diagram for QC phase formation. Therefore, the parameters by which one can control this relationship are (1) the diameter of the sample for controlling cooling rate, and (2) the content of the dominant elements for the nose position of the TTT curves. In addition, it is considered that (3) hydrostatic pressure can influence the nucleation behavior of the QC phase. There are some reports discussing the pressure effect on glass transition and nanocrystallization in metallic glasses during heating from a glassy solid to the supercooled liquid (SCL).[8,9] During the cooling from SCL to a glassy solid, the precipitation may depend more on pressure because SCL with a low viscosity near the liquidus temperature (T_l), is more sensitive to pressure than that with a high viscosity near the glass transition temperature (T_g).

Here, we report the influences of sample diameter (D), Pd content (x), and hydrostatic pressure (P) in a chamber during casting on the structure of as-cast $Zr_{65}Al_{7.5}Ni_{10}Cu_{17.5-x}Pd_x$($x=10, 17.5$ at.%) bulk alloys. The results indicate that TTT-curves for QC phase formation and the subsequent equilibrium phases shift to the shorter time side with decreasing P, and the pressure sensitivity of QC phase formation increases with x.

Master ingots were produced by arc-melting high-purity metal elements (99.9% for Zr, and 99.99% for others). These alloys were heated by an induction melting method up to 1223 K±3 K under vacuum ($P\sim 4\times 10^{-3}$ Pa) or atmospheric pressures ($P\sim 0.1$ MPa) of purified argon inert gas. Then the melts were cast into rods of $D=2$ and 3 mm, 50 mm in length. The temperature of the melts was monitored using a pyrometer. The oxygen concentrations in the $Zr_{65}Al_{7.5}Ni_{10}Pd_{17.5}$ rods cast at $P=0.1$ MPa and 4.0×10^{-3} Pa were found to be 200 and 167 ppm, respectively. The structure of the samples was examined by x-ray diffraction (XRD) analysis with CuKα radiation and by field-emission transmission electron microscopy (JEOL, JEM3000F) with an acceleration voltage of 300 kV. The thermal properties of the samples were examined by differential scanning calorimetry (DSC) at a heating rate of 0.083 K/s with alumina crucibles.

Figure 1(a) shows the XRD patterns of the $Zr_{65}Al_{7.5}Ni_{10}Cu_{7.5}Pd_{10}$($x=10$) alloys of $D=3$ mm cast at $P\sim 0.1$ MPa and $\sim 4\times 10^{-3}$ Pa, and of $D=2$ mm cast at $P\sim 4\times 10^{-3}$ Pa; hereafter, we designated these samples 10Pd3A, 10Pd3V, and 10Pd2V, respectively. The XRD pattern of 10Pd3A shows only a halo pattern which is characteristic of a glassy structure, while that of 10Pd3V consists of broad peaks of the tetragonal-Zr_2Ni phase which has been previously observed in annealed Zr_2Ni melt-spun ribbons.[10] Figure 1(b) shows the XRD patterns of the $Zr_{65}Al_{7.5}Ni_{10}Pd_{17.5}$($x=17.5$) alloys of $D=3$ mm cast at $P\sim 0.1$ MPa and $\sim 4\times 10^{-3}$ Pa, and $D=2$ mm at $P\sim 4\times 10^{-3}$ Pa; hereafter, we designated these samples 17.5Pd3A, 17.5Pd3V, and 17.5Pd2V, respectively. The XRD pattern of 17.5Pd3A shows only a halo pattern, while that of 17.5Pd3V consists of peaks of the QC phase. Figures 2(a)

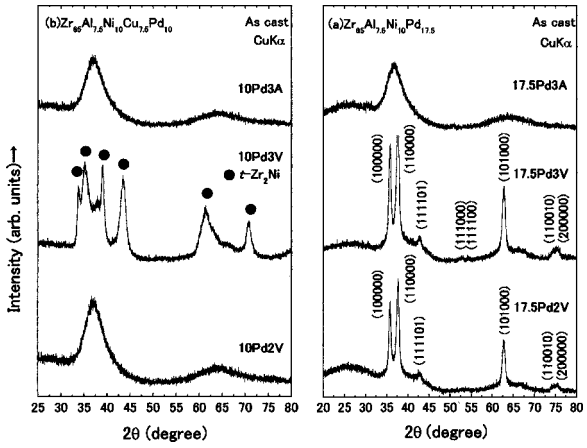

FIG. 1. (a) XRD patterns of $Zr_{65}Al_{7.5}Ni_{10}Cu_{7.5}Pd_{10}$ ($x=10$) alloys of 3 mm ϕ cast at chamber pressure of $P\sim0.1$ MPa (10Pd3A), $\sim4\times10^{-3}$ Pa (10Pd3V), and of 2 mm ϕ cast at $P\sim4\times10^{-3}$ Pa (10Pd2V). (b) XRD patterns of $Zr_{65}Al_{7.5}Ni_{10}Pd_{17.5}$ ($x=17.5$) alloys of 3 mm ϕ cast at $P\sim0.1$ MPa (17.5Pd3A), $\sim4\times10^{-3}$ Pa (17.5Pd3V), and 2 mm ϕ at $P\sim4\times10^{-3}$ Pa (17.5Pd2V).

and 2(b) show bright-field TEM images of 17.5Pd3A with a selected-area electron diffraction pattern and those of 17.5Pd3V with a nanobeam diffraction pattern, respectively. One can confirm that 17.5Pd3A exhibits a glassy phase, but 17.5Pd3V consists mainly of QC precipitates with an average diameter less than 50 nm. The rod diameters of 17.5Pd3A, 17.5Pd3V, 10Pd3A, and 10Pd3V are 3 mm. Therefore, the cooling rates are considered to be approximately the same for these cast alloys because the heat transfer of the mould cast method is achieved through the copper walls and the contribution of the atmospheric inert gas can be neglected. However, for the two compositions, $x=10$ and 17.5, the samples cast at $P\sim0.1$ MPa are of the single glassy phase, while those cast at $P=4\times10^{-3}$ Pa contains the crystalline phases. Therefore, one can conclude that this difference in as-cast structure is due to the difference in hydrostatic pressure in the chamber. The decrease in P during the casting process decreases GFA, i.e., it enhances the devitrification in this alloy system.

Figure 3(a) shows the DSC curves for 10Pd3A, 10Pd3V, and 10Pd2V, and Fig. 3(b) those for 17.5Pd3A, 17.5Pd3V, and 17.5Pd2A. According to the reports on $Zr_{65}Al_{7.5}Ni_{10}Pd_{17.5-x}Pd_x$ ($x=5-17.5$) by Saida *et al.*,[11] the first exothermic peak is due to the nanoquasicrystallization in

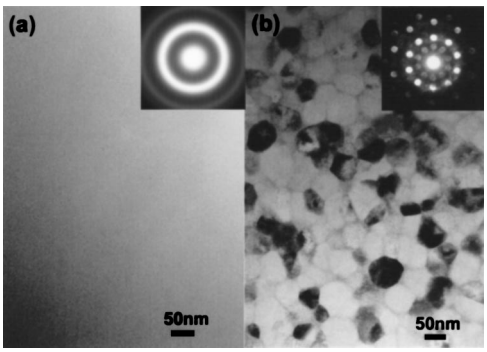

FIG. 2. Bright-field TEM images of $Zr_{65}Al_{7.5}Ni_{10}Pd_{17.5}$ ($x=17.5$) alloys of 3 mm ϕ cast at chamber pressures (a) $P\sim0.1$ MPa (17.5Pd3A) and (b) $P\sim4\times10^{-3}$ Pa (17.5Pd3V), with selected area electron diffraction pattern (SADP) and nanobeam (beam diameter =2.4 nm) diffraction pattern are inserted, respectively.

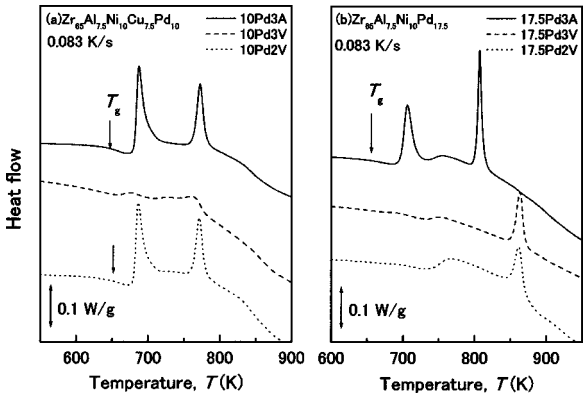

FIG. 3. (a) DSC curves of the $Zr_{65}Al_{7.5}Ni_{10}Cu_{7.5}Pd_{10}$ ($x=10$) alloys of 3 mm ϕ cast at the chamber pressures of $P\sim0.1$ MPa (10Pd3A), $\sim4\times10^{-3}$ Pa (10Pd3V), and of 2 mm ϕ cast at $P\sim4\times10^{-3}$ Pa (10Pd2V). (b) DSC curves of the $Zr_{65}Al_{7.5}Ni_{10}Pd_{17.5}$ ($x=17.5$) alloys of 3 mm ϕ cast at $P\sim0.1$ MPa (17.5Pd3A), $\sim4\times10^{-3}$ Pa (17.5Pd3V), and of 2 mm ϕ at $P\sim4\times10^{-3}$ Pa (17.5Pd2V).

SCL and the second one is due to the subsequent transformation from the QC phase to the equilibrium phase, e.g., tetragonal-Zr_2Ni, Zr_2Cu, etc. The first exothermic peak in the DSC curve for 17.5Pd3V whose XRD pattern [Fig. 1(b)] shows the existence of the QC phase completely disappears, but the second one remained. On the other hand, not only the first peak but also the second peak almost disappears in 10Pd3V. Therefore, we have observed the tetragonal-Zr_2Ni equilibrium phase in 10Pd3V [Fig. 1(a)].

Hydrostatic pressure may influence the thermodynamic potential energy barrier of nucleation in the SCL region during cooling. The nucleation rate I is expressed by

$$I=\frac{I_0}{\exp\left(\dfrac{\Delta G^*+Q_n}{k_BT}\right)}, \tag{1}$$

where I_0, k_B, Q_n, and ΔG^* are a constant, Boltzmann's constant, the activation energy for the transport of an atom across the interface of an embryo, and the free energy required to form a nucleus of critical size, respectively. The dependence of external pressure on the devitrification of SCL during heating is discussed in some reports. According to Jiang *et al.*,[12] the nucleation work, ΔG^*+Q_n, can be influenced by external pressure. ΔG^* is proportional to $\sigma^3/(p\Delta V+\Delta G)^2$, where σ, ΔV, and ΔG are the interfacial energy of the crystal, molar volume, and free-energy changes from SCL to the crystalline phase, respectively. σ and ΔG are considered to be independent of external pressure. In general, the increase in hydrostatic pressure reduces atomic mobility, and therefore, Q_n increases. The pressure effect on ΔG^*+Q_n in SCL could be determined by ΔG^* and Q_n, therefore the sign of ΔV. In the case of the Zr-Al-Ni-Cu-Pd system, its GFA increases with increasing P [Fig. 1(b)]. This result allows the sign of ΔV to be both positive and negative. However, Holzer and Kelton[13] and Jiang *et al.*[12] reported an increase in molar volume by the quasicrystallization of the $Al_{75}Cu_{15}V_{10}$ and $Zr_{70}Pd_{30}$ alloys, respectively. We can fairly assume that the sign of ΔV ($=V_{QC}-V_{scl}$) for the Zr-Al-Ni-Cu-Pd metallic glass is positive. Therefore, both ΔG^* and Q_n increase with increasing external pressure. However, $P\Delta V$ may be much smaller than ΔG, therefore ΔG^* varies little at $P=0.1$ MPa and 4×10^{-3} Pa. The reason why

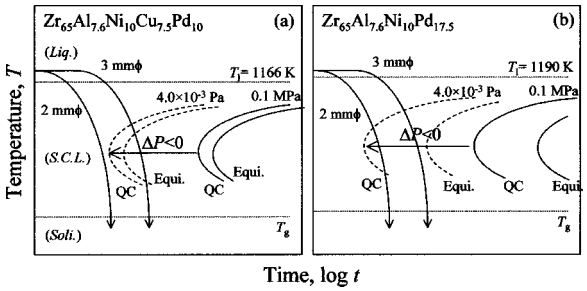

FIG. 4. Schematic illustrations of cooling route of cast rods 2 and 3 mm in diameter in TTT diagrams for (a) $Zr_{65}Al_{7.5}Ni_{10}Cu_{7.5}Pd_{10}$ and (b) $Zr_{65}Al_{7.5}Ni_{10}Pd_{17.5}$ alloys. Curves with dotted and solid lines are TTT curves at chamber pressures P of $\sim 4\times 10^{-3}$ Pa and of 0.1 MPa, respectively. Curves with QC and equi. notations are TTT curves for the formation of quasicrystalline and equilibrium phases, repectively.

the chamber pressure strongly influences the nucleation behavior in the alloys is not cleared in this letter.

Incubation time for the nucleation could be the inverse of the nucleation rate, I^{-1}; thus it increases with decreasing temperature. Meanwhile, the viscosity of SCL increases according to the Vogel-Fulcher-Tammann formula[14] and the corresponding relaxation time, τ, increases with decreasing temperature. Therefore, during the cooling, the precipitation of the primary phase and the vitrification of alloy melt are competing phenomena. If I^{-1} maintained larger than τ, SCL finally freezes into a single-glassy phase at T_g; otherwise, the precipitation occurs during the cooling. To investigate the influence of cooling rate on the structure of as-cast $Zr_{65}Al_{7.5}Ni_{10}Cu_{17.5-x}Pd_x$ ($x=10, 17.5$ at.%) alloys, the XRD and DSC results of the samples of $D=2$ mm are shown in Figs. 1 and 3, respectively. 17.5Pd2V was mainly of the QC phase, the same as 17.5Pd3V, i.e., $I^{-1}<\tau$, on the other hand, 10Pd2V froze into a single glass, i.e., $I^{-1}>\tau$.

Based on the above results, schematic illustrations of the cooling route in the TTT curves are summarized in Figs. 4(a) and 4(b) for the 10Pd and 17.5Pd series, respectively. Because the reduced glass-transition temperatures, T_g/T_1, of these two alloys are almost the same at ~ 0.55, the TTT curves of the primary QC phase for these alloys at $P=0.1$ MPa can be drawn at almost the same time positions [see solid lines in Figs. 4(a) and 4(b)], respectively. In addition, the time interval between the primary QC phase formation and the subsequent equilibrium (equi.) phases should be larger for 17.5Pd and smaller for 10Pd [see solid lines in Figs. 4(a) and 4(b)] because the thermal stability of the QC phase increases with Pd content.[2,11] The TTT curves of the QC and equi. shift to the shorter time side with decreasing P and are drawn by dotted lines. Considering the results in Figs. 1 and 3, the nose points of the QC and Equi. curves at $P=4\times 10^{-3}$ Pa should be placed between the cooling lines of $D=2$ and 3 mm for the 10Pd alloy in Fig. 4(a). On the other hand, these cooling lines should be placed between the nose points of the QC and equi. curves for the 17.5 Pd alloy in Fig. 4(b). These results indicate that the influence of pressure on TTT curves increases with increasing Pd content.

In summary, the influences of sample diameter, Pd content, and hydrostatic pressure in a chamber during the casting on the structure of as-cast $Zr_{65}Al_{7.5}Ni_{10}Cu_{17.5-x}Pd_x$ ($x=10, 17.5$ at.%) bulk alloys were investigated. It is concluded that the nose position of TTT-curves for icosahedral and subsequent equilibrium phases shift to a shorter time side with decreasing hydrostatic pressure in the chamber during casting. The pressure sensitivity of icosahedral phase formation increases with Pd content. Lastly, the control of hydrostatic pressure during casting may open up fabrication processes for bulk metallic glasses and bulk nanostructured alloys.

[1] M. W. Chen, T. Zhang, A. Inoue, S. Sakai, and T. Sakurai, Appl. Phys. Lett. **75**, 1697 (1999).
[2] A. Inoue, T. Zhang, J. Saida, M. Matsuhista, M. W Chen, and T. Sakurai, Mater. Trans., JIM **40**, 1181 (1999).
[3] U. Koester, J. Meinhardt, S. Roos, and H. Lieberts, Appl. Phys. Lett. **69**, 179 (1996).
[4] J. Saida, M. Matsushita, C. Li, and A. Inoue, Appl. Phys. Lett. **76**, 3558 (2000).
[5] M. Matsushita, J. Saida, C. Li, and A. Inoue, J. Mater. Res. **15**, 1280 (2000).
[6] J. Saida, M. Matsushita, and A. Inoue, J. Appl. Phys. **90**, 4717 (2001).
[7] B. S. Murty and K. Hono, Appl. Phys. Lett. **84**, 1674 (2004).
[8] J. Z. Jiang, J. S. Olsen, L. Gerward, S. Abdali, J. Eckert, N. Schlorke-de Boer, L. Schlutz, J. Truckenbrodt, and P. X. Shi, J. Appl. Phys. **87**, 2664 (2000).
[9] P. F. Xing, Y. X. Zhuang, L. Gerward, and J. Z. Jiang, J. Appl. Phys. **91**, 4956 (2002).
[10] C. Li, J. Saida, M. Matsushita, and A. Inoue, Mater. Lett. **44**, 80 (2000).
[11] J. Saida, M. Matsushita, and A. Inoue, Mater. Trans., JIM **41**, 1505 (2000).
[12] J. Z. Jiang, S. Jeppesen, J. Saida, and C. Lathe, J. Appl. Phys. **95**, 4651 (2004).
[13] J. C. Holzer and K. F. Kelton, Acta Metall. Mater. **39**, 1833 (1991).
[14] R. Busch, E. Bakke, and W. L. Johnson, Acta Mater. **46**, 4725 (1998).